Chapter 5

1D Titania Nanoarchitecture as Bioactive and Photoactive Coatings for Modern Implants: A Review

Aleksandra Radtke

Additional information is available at the end of the chapter

http://dx.doi.org/10.5772/intechopen.69138

Abstract

The research efforts in understanding the influence of TiO_2 1D nanoarchitecture structure and morphology on its biological and photocatalytic activity absorbed a lot of attention during last few years. Nowadays, the application of TiO_2 coatings in biomedical technologies (e.g., in modern implantology) requires the material of strictly defined structure and morphology, possessing both high biocompatibility, as well as antimicrobial properties. The presented review is a compilation of interdisciplinary knowledge about the application of 1D TiO_2 nanostructural coatings (nanotubes, nanofibres, nanowires) in biomedical technologies. The methods and parameters of their synthesis, and the physicochemical techniques used in the characterization of their structure and morphology, are discussed. Moreover, their ability to be applied as innovative coatings for modern implants is presented.

Keywords: 1D nanoarchitecture, TiO_2, nanotubes, nanofibers, nanowires, implant

1. Introduction

The use of modern materials in biomedical technologies requires detailed knowledge on the impact of the structure and the physicochemical properties of produced systems on their bioactivity. There are a lot of biomaterials, which can be applied in the human body, such as metals, ceramics, synthetic and natural polymers [1–8]. Among them titanium and its alloys have become extremely popular, especially in the implantology [9–15]. Commercially pure titanium (cpTi) is one of the dominant materials used for dental implants [16–20]. Ti6Al4V alloy plays an important role for orthopaedic applications [21–25]. Nickel-titanium alloy (Nitinol, shape memory alloy) has been used in the treatment of cardiovascular implants [26–30]. The combination

of the high corrosion resistance, the tensile strength, the flexibility, and the biocompatibility, is the reason of widespread and successful application of titianium and its alloys in modern implantology [31–34]. The mentioned outstanding corrosion resistance of Ti and its alloys is a consequence of the passivation oxide layer spontaneous formation. This oxide layer is in fact responsible for the biocompatibility of Ti/Ti alloy. The thickness and the composition of natural oxide coatings, which appear in the presence of air or oxidizing media, and which are based on mainly TiO_2, Ti_2O_3 or TiO, depend on the environmental conditions [13–15, 35–37]. However, the stoichiometric defects and the low stability of this film can lead, in the case of implants, to their delamination and loosening. The key parameter in the success of bone implants (orthopaedics and dentistry) and the clinical goal is the establishment of a strong and long-lasting connection between the implant surface and peri-implant bone, in other word, achieving the optimal osseo-integration [38–43]. Even if Ti and its alloys are biocompatible materials, as they are biostable and biologically inert, the human body recognizes them as foreign ones and tries to isolate them using thin nonmineral, soft tissue layer. Instead, the mechanical interlocking of the titanium surface asperities and the bones pores leads to the formation of the bond between the implant and the bone, that is to the successful osseointegration [44–47]. The mechanical, chemical, and physical methods have been reported to improve the bioactivity of titanium and the bone conductivity (**Table 1**) [12, 48–81].

Modification method	Modified surface layer	The aim of modification	Ref.
Mechanical methods			[12]
Machining	Rough or smooth surface formed by subtraction process	Production of the specific surface topography; surface cleaning and roughening, improvement of adhesion in bonding	[49]
Grinding			[50–52]
Polishing			[53]
Blasting			[50, 51, 54, 55]
Chemical methods			[48]
Acidic treatment	<10 nm of surface oxide layer	Removal of oxide scales and contamination	[56, 57]
Alkaline treatment	~1 μm of titanate gel	Improvement of biocompatibility, bioactivity and bone conductivity	[57, 58]
H_2O_2 treatment	~5 nm of dense inner	Improvement of biocompatibility, bioactivity and bone conductivity	[59]
Sol-gel	~10 μm of thin film, such as calcium phosphate, TiO_2 and silica	Improvement of biocompatibility, bioactivity and bone conductivity	[60–62]
Anodic oxidation	~10 nm to 40 μm of TiO_2 nanotubular or porous layer, adsorption and incorporation of electrolyte anions	Production of the specific surface topography; improvement of biocompatibility, bioactivity and bone conductivity, improvement of corrosion resistance	[63–66]
CVD (chemical vapor deposition)	~1 μm of TiN, TiC, TiCN, diamond and diamond-like carbon thin films	Improvement of wear resistance, corrosion resistance, and blood compatibility	[67–69]

Modification method	Modified surface layer	The aim of modification	Ref.
Biochemical methods	Modification through silanized titania, photochemistry, self-assembled monolayers	Inducing the specific cell and tissue response by means of surface immobilized peptides, proteins, or growth factor	[70, 71]
Physical methods			[48]
Thermal spray Flame spray Plasma spray	~30 μm–200 μm of coatings such as titanium, hydroxyapatites, calcium silicates, Al_2O_3, ZrO_2, TiO_2	Improvement of wear resistance, corrosion resistance, and biological properties	[72–76]
Physical vapor deposition Evaporation Ion plating Sputtering	~1 μm of TiN, TiC, TiCN, diamond, and diamond-like carbon thin film; hydroxyapatite coating by sputtering	Improvement of wear resistance, corrosion resistance, and blood compatibility	[77, 78]
Ion implantation and deposition	~10 nm of surface modified layer	Modification of surface composition, improvement of wear resistance, corrosion resistance, and biocompatibility	[79, 80]
Glow discharge plasma treatment	~1 to ~100 nm of surface modified layer	Cleaning, sterilization, and oxidation of the surface, surface nitridation, removal of the native oxide layer	[81, 82]

Table 1. Overview of surface modification methods for Ti and Ti alloys.

A review of the Ti/Ti alloys surface chemical modification processes, which led to the formation of 1-D titanium dioxide nanostructures and improve the bioactivity of modified titanium materials, is the aim of this chapter. The relationship between the structure and the morphology of titania nanotubes (TNT), titania nanofibres (TNF), and titania nanowires (TNWs) and their bioactivity is discussed in the next subsections. Moreover, it cannot be forgotten that from chemical point of view, described 1D titania nanostructures are in the whole sense of the word, TiO_2, which is very known semiconducting photocatalyst. So, the aspects associated with the photoactivity of TNT, TNF, and TNW coatings are also discussed. This feature of titania can be treated as additional attribute to use, for example, in the process of implant surface antibacterial disinfection, with the use of UV light. But, the reader should bear in mind the fact that the photoactivity of TiO_2 is strongly dependent on its structure and morphology.

2. Structural characterization of 1D titania coatings

Titania is well known to exist mainly in three crystalline modifications: tetragonal rutile, tetragonal anatase, and orthorhombic brookite [82]. The structure of the titania lattice is determined by the way in which TiO_6 octahedra are linked [83]. These polymorphic forms of TiO_2 characterize

different structural stability, different photo- and bioactivity, as well as different electrical and optical properties [84–86]. This fact causes that the determination of the structure of materials basing on TiO_2 is especially important for their further, for example, biomedical, applications.

In order to determine the titania structure, X-ray diffraction studies are often carried out. Characteristic set of 2Θ [°] signals: 25.33 (101), 37.80 (004), 48.08 (200), 55.12 (211) indicates the presence of anatase form, whereas the signals: 27.50 (110), 36.17 (101), 41.50 (111), 54.46 (211) prove that rutile form is our studied sample [87–90].

Raman spectroscopy is another very useful method to recognize and characterize the titania structures. Basing on the group analysis, there are six active Raman modes (A_{1g}, $2B_{1g}$, $3E_g$) for anatase D_{4h} ($I4_1/amd$) and four active Raman modes (A_{1g}, B_{1g}, $B_{2g,}$ and E_g) for rutile D_{4h} ($P4_2/mnm$) [91, 92]. According to previous reports, the set of bands, which appear in Raman spectra at 197, 339, 519 and 639 cm^{-1}, indicates the formation of TiO_2 anatase form. For TiO_2 rutile form, the base of identification is the detection of bands at 447 and 612 cm^{-1} [91–94]. It should be pointed out that very often the fabrication of materials based on TiO_2 on nanoscale causes the formation of amorphic systems or amorphic systems containing small amount of crystalline phases [95, 96]. In such cases, Raman mapping of whole sample surface can help in the detailed determination of the structure.

The structure of thin titania films can be determined by the use of transmission electron microscopy studies, on the base of selective area electron diffraction (SAED) and the determination of *d*-spacing from HRTEM images of nano-TiO_2-sample [97, 98].

The use of mentioned in this subsection instrumental methods led to state about the structure of 1D-titania nanostructures. Even if they are not perfectly crystalline just like in case of amorphous samples possessing some crystalline islands in the structure.

3. Titania nanotubes (TNTs)

The choice of titania nanotubes as the first of the described 1D-titania nanostructures is not accidental, as the methodology of their production is well known. The electrochemical oxidation process of Ti and Ti alloys, in which TiO_2 nanotubes are produced, is one of the most popular methods to produce controlled and strictly defined structures on the surface of implants [99–106]. Sol-gel techniques, hydrothermal and solvothermal methods with or without templates, and atomic layer deposition (ALD) into the template are among other methods used in the production of TiO_2 nanotubes [107–111]. However, tailoring the process conditions and the possibility to obtain strictly defined morphology of nanotubes, caused that electrochemical anodization of titanium substrate, is particularly actively reviewed and practically used [67, 112–115]. The anodic oxidation process includes electrode reactions and metal and oxygen ions diffusion. The combination of these actions leads to the formation of oxide layer on the surface of Ti/Ti alloy, which acts as an anode (**Figure 1**).

This process is usually carried out by applying a constant voltage between 1 and 30 V in aqueous electrolyte or 5–150 V in nonaqueous electrolytes, containing in both cases approximately

http://dx.doi.org/10.5772/intechopen.69138

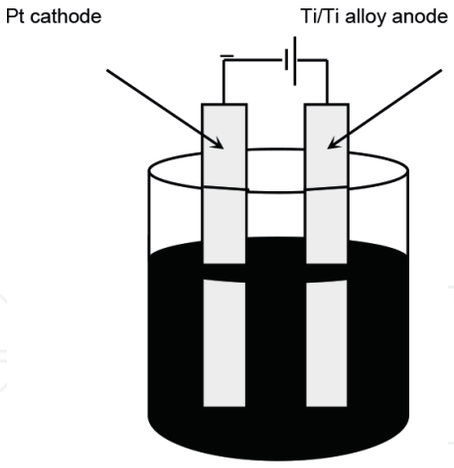

Figure 1. Scheme of the anodization setup.

0.1–1wt% fluoride ions. The presence of F^- ions in the electrolyte is absolutely essential, as they are, in fact, responsible for the creation of nanotubes morphology. Without them, a compact oxide layer would be formed on the titanium surface. Fluorides form water-soluble $[TiF_6]^{2-}$ species, both in the process of the complexation, which occurs with Ti^{4+} ions ejected at the oxide-electrolyte interface as well as by chemical attack of the formed TiO_2. The fluoride concentration is crucial for this process, and up to it, three very different electrochemical characteristics can be obtained. In case of fluoride content ≤0.5 wt%, stable compact oxide layer is formed. If the concentration is high, approximately 1 wt%, no oxide formation is observed, as all the Ti^{4+} ions formed in the oxidation of Ti, immediately react with the abundant fluorides, forming soluble complex anions $[TiF_6]^{2-}$. And for intermediate fluoride concentrations, between 0.5 wt% and 1 wt%, porous oxide or nanotubes formation can be observed as a consequence of a competition between oxide formation and Ti^{4+} solvatization [116, 117].

By tailoring the anodization parameters, such as applied voltage, anodization time, and concentrations of chemicals, TiO_2 nanotubes of different diameters (from 15 nm up to 300 nm) and lengths are possible to obtain (**Figure 2**a). And in such stable conditions, regular nanoscope pores/tubes, open on the top and close at the bottom, are formed. Our studies showed that the use of very small potential (below 4 V) led to the formation of regularly nanoporous coatings. The use of the potential from the region 4–12 V led to the creation of nanotubular coatings, in which nanotubes still posses common walls. Only the use of potential higher than 12 V gave the coatings composed of independent and separated nanotubes (**Figure 2**b–d) [118].

Some modifications in the tube geometry can be achieved by changing the anodization voltage during the tube growth process. Applying voltage steps, pulsing between two appropriate voltages can be used to generate tube stacks, bamboo nanotubes, or nanolaces [119–121]. The use of organic electrolytes, such as ethylene glycol, DMSO, glycerol, or ionic liquids, leads to the formation of nanotubes of different morphology and composition. The presence of lower water content in the electrolyte, which controls tube splitting, determines the synthesis of coatings with very long tubes and smooth walls, as well as with large diameters (up to 700 nm) [122–125].

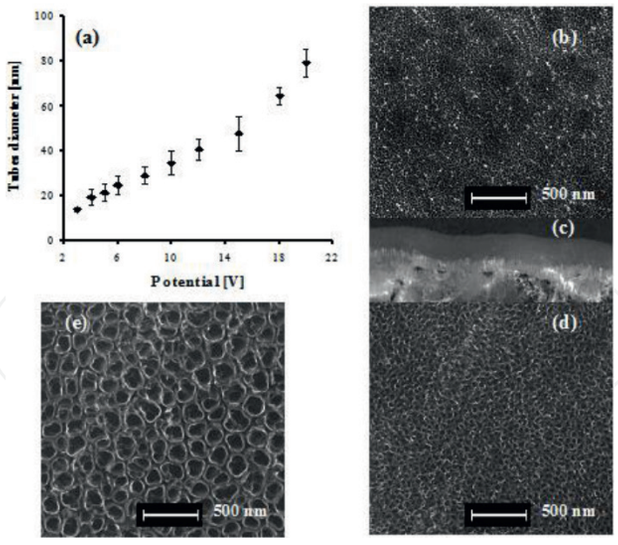

Figure 2. (a) The dependence between the applied voltage and diameter of nanotubes, SEM images of TNT3 (b), TNT10 (c), and TNT18 (d).

Regardless of whether an aqueous or nonaqueous electrolyte was used in the anodic oxidation process, TiO_2 nanotubes product is typically amorphous. It is necessary to anneal them in order to obtain crystalline product. Phase transformation to anatase takes place at 300–400°C, and from anatase to rutile at temperatures 500–700°C. Elevated temperatures (700–800°C) lead to the sintering and the collapsing of TNT [126]. The conversion temperature is strictly dependent on the several factors, such as nanotubes diameter, morphology, and impurities. It was proved that for small diameters (below 30 nm) rutile rather than anatase appears during annealing of amorphous nanotubes. Moreover, our studies showed that at very low potential (5 V), it was possible to obtain product in the rutile form, without annealing the sample. Both GAXRD and HRTEM proved this polymorphic form [118].

Taking into account the fact that titania nanotube arrays are one of the most promising candidates for coating of Ti and Ti alloys surface in implants fabrication (even for 3-D implants, as it can be seen in **Figure 3**), it is worth to consider the TNT structure and morphology impact on the cellular response.

There is a clear effect of the TNT diameter on the cell adhesion, proliferation and differentiation. Diameters of 15–20 nm are optimal and in case of such TNT presence on the surface of titanium implants, increase in adhesion and proliferation of several types of living cells, such as fibroblasts, osteoblasts, osteoclasts, mesenchymal stem cells, hematopoietic stem cells, and endothelial cells, was confirmed [127–134]. Higher tube diameters (>100 nm) have no positive influence on the increasing of adhesion or proliferation and some authors have shown that TNT of such diameters led to apoptosis, i.e., programmed cell death [135]. The size effect can be explained by the fact that integrin clustering in the cell membrane leads to a focal adhesion complex with the size of about 10 nm in diameter, perfectly fitted to nanotubes with about 15 nm diameters [134]. Gongadze et al. suggest that nanorough titanium surfaces with edges and spikes could promote the adhesion of living cells, especially osteoblasts [129].

http://dx.doi.org/10.5772/intechopen.69138

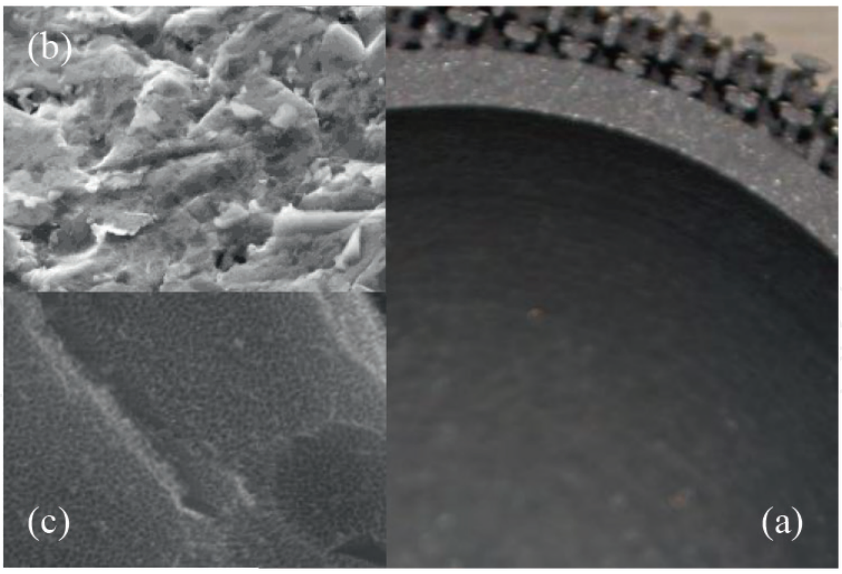

Figure 3. The surface of 3-D implant (a), uncoated (b) and coated by nanotubes (c).

A small diameter nanotube surface has more sharp convex edges per unit area than a large one. This fact can explain stronger cellular binding affinity on the surface of small diameter nanotubes, than on the surface of TNT with larger diameters. All studied samples mentioned above were annealed before carrying the adhesion and proliferation studies, so they were in crystalline form, mostly in anatase form. In our work, we studied the biological answer of as-obtained nanotubes, mostly amorphous, containing crystalline islands. We have noticed that even without further annealing, titania nanotubes showed better osseointegration than pure titanium. The adhesion and the proliferation of fibroblasts were different for the nanotubes of different diameters. The best biological answer was visible for nanotubes obtained at 5 V, whose diameters were ~20 nm [136]. This result is in accordance with earlier reports [127–134], however, our investigations revealed that the annealing of amorphous samples was not so indispensable [136].

Successful osseointegration is an important clinical goal but the important thing is the reduction of the bacterial biofilm formation on the surface of implant. Regardless of the type of biomaterial used, the initial inflammation response is always present and it may turn into an acute inflammation or even chronic inflammation. So, it is not surprising that the possibilities of a bacteria-repellent surface modification are investigated. Literature data and own studies showed that controlled diameter nanotubes displayed significantly changed responses to *Staphylococcus aureus* and *Staphylococcus epidermis* [137–140]. The size-effect exists for bacteria but also the structure of TNT influences the direction of the changes. According to Puckett et al., the use of larger diameter nanotubes decreased the number of live bacteria as compared to lower diameter ones and pure titanium [141]. But it is worth to know that analyzed nanotubes coatings were crystalline, in the form of anatase, as they were posttreated after anodization process by annealing. According to results of studies on amorphic nanotubes, which were not postannealed, the best antibacterial properties against *S. aureus* were seen for the nanotubes with small diameter but possessing the rutile form [118].

TiO_2 is one of the most photocatalytically active material used to decompose the organic pollutants and also bacteria [142–145]. The reason for this high activity is the band-edge positions in relation to typical environments, for example H_2O. The energy band gap is adequate to the ultraviolet light energy and UV light promotes electrons from the valence band to the conduction band. As a result, the holes are formed in the valence band. Separated holes and electrons reach the semiconductor-environment interface, and react with appropriate redox species. Because of water presence, several highly reactive species are generated by charge exchange at the valence band ($H_2O + h^+ \rightarrow OH^\bullet$) and at the conduction band ($O + e^- \rightarrow O_2^-$). These radicals and peroxo ions are able to virtually oxidize all organic materials to CO_2 and H_2O. Furthermore, at the valence band, direct h^+ transfer to adsorbed species to initiate the decomposition may also be considered [146–150].

It should be pointed out that in all of the photocatalytic applications, a higher overall reaction rate is achieved using high-surface-area geometries. Ordered nanotube arrangements offer various advantages over nanoparticulate assemblies, as their defined geometry provides strictly determined retention times in nanoscopic photoreactors. Moreover, the 1-D geometry may allow a fast carrier transport and thus less unwanted recombination losses [151, 152].

The earlier researches showed that TiO_2 nanotube coatings can indeed have the higher photocatalytic reactivity than a comparable nanoparticulate layer. The optimized reaction geometry for charge transfer, UV absorption characteristics over the tube, and solution diffusion effects are the main factors, which may be responsible for this effect. They allow an improved photoabsorption, longer electron lifetime, and diffusion length in TiO_2 nanotubes in comparison with nanoparticles [152, 153]. Photoactivity of TNT depends on the dimensions and wall thickness of the nanotubes, their crystallinity, and their packing density, because the separation and transport of charge, as well as the grain boundary effect, would greatly hinge on such factors [154]. It was shown that silver or gold particle decoration led to a significantly higher photocatalytic activity [155]. The same increasing of photoactivity was also obtained by applying an external anodic voltage [156]. These facts suggest that in case of investigated objects, a valence-band mechanism dominates, and the observed accelerating effects have a common origin in increased band bending, either by applied voltage or by the junction formation [157].

Our studies showed that amorphic titania nanotubes possessing some crystalline impurities indicated very high photoactivity in the reaction of methylene blue and acetone degradation in the presence of UV light [118]. The clear influence of the tubes diameter, and at the same time, of specific surface area, on the value of observed rate constants, was also visible. Additional information which we have obtained from our research was the fact that it was not possible to make a clear comparison of TNT photoactivity in the degradation of different organic pollutant patterns (water-soluble methylene blue and volatile aceton), as the mechanisms of their degradation were completely different and they depended on variable parameters (the size of pattern molecules which affects the reactant molecule adsorption, pH of solution). However, the surface of the implant modified by anodic oxidation can possibly be disinfected/sterilized only with the use of UV light, as it reveals higher activity than unmodified Ti surface possessing only the natural passivation oxide film. It is an important property because the same coating plays a dual role for the implants—increases osseointegration process and creates optimal conditions for carrying out the process of implant surface sterilization/disinfection with the use of UV light.

http://dx.doi.org/10.5772/intechopen.69138

4. Titania nanofibrous coatings (TNFs)

The electrospinning is a technique mostly used in the fabrication of the TNF coatings [158–160]. It is a very simple and convenient method for the preparation of polymer fibers and ceramic fibers, which are extremely long, uniform in diameter, raging from tens nanometer to several micrometers, and diversified in compositions [161]. The electrospinning process involves a high voltage source connected to a needle and a metallic collector where the fibers are deposited. The needle, which is attached to injection pump, represents the positive electrode. The collector is connected to the negative electrode, thus creating a potential difference. Electric field created in this way stretches the drop that forms on the needle tip, which is then deformed into a conical shape (Taylor cone). When the applied electric field exceeds the surface tension of the drop, the solution is ejected in the form of an electrically charged jet, reaching the negative electrode, which is the collector. During this process, the solvent is evaporated resulting in the deposition of nanofibers over the collector. The diameter of the fibers can be adjusted by varying the rheological properties of the solution and turning the processing parameters [162, 163]. The scheme of the electrospinning setup is given in **Figure 4**. Electrospun TiO_2 nanoarchitecture is formed by electrospinning titania precursor (e.g., titanium(IV) alkoxides) along with adequate polymer and subsequent polymer burning in high temperature sintering process. The synthesis involves the following four steps: (1) the preparation of the titania precursor sol, (2) mixing of the sol with the polymer template to obtain the solution for electrospinning, (3) electrospinning of the solution with the use of the apparatus showed in **Figure 4**, and (4) the calcination of as-prepared TNF to obtain crystalline titania nanofibers [164]. The morphology and the diameter of the electrospun titania depend on the following parameters related to: (a) the solution, (b) the process, and (c) the ambient (**Table 2**), while the structure of formed nanofibers is strictly associated with the postcalcination process [165–173].

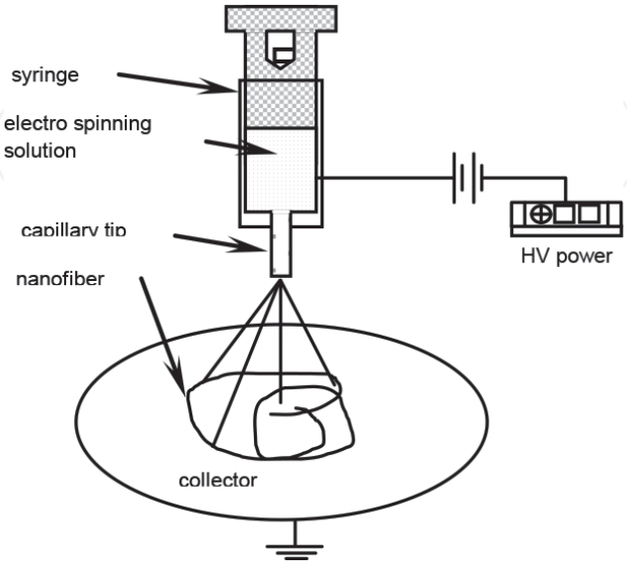

Figure 4. Scheme of electrospinning setup.

Parameter	Effect on TNF morphology	Ref.
Solution parameters		
Polymer concentration	Increase in TNF diameter with increase of polymer concentration	[165–167]
Titania precursor concentration	Increase in TNF diameter with increase of titania precursor concentration	[165, 166, 168, 169]
Viscosity	Low viscosity leads to bead formation, higher viscosity leads to disappearance of bead but nanofiber with larger diameter is produced	[165,170]
Solvent volatility	High volatility leads to formation of nanofiber in concave morphology	[171]
Dielectric constant	Low dielectric constant results in the formation of larger size nanofibers	[171]
Processing parameters		
Applied voltage, electric field	TNF diameter decreases with increasing applied voltage; when the applied voltage is above 1.6 kV/cm, the diameter increases, because of the jet instability	[165, 166]
Feeding rate	Increase in feeding rate results in the increase of nanofiber diameter	[165]
Collector geometry	The geometry affects the directionality of the formed nanofibers	[170]
Ambient parameters		
Calcination temperature	Higher temperature results in the reduction of nanofiber size, because of the loss of polymer and the crystallization process of titania	[165, 168, 171–173]

Table 2. Summarization of the electrospinning parameters affected the nanofibers morphology.

Another technique to produce titania nanofibrous coatings is the laser ablation, proposed by Tavangar et al. [174]. During the laser irradiation of titanium substrate, the illuminated region is heated up and vaporized, producing the plasma plume. The plume expands outwards and its temperature and pressure decreases. The next process is the condensation of plasma plume leading to the formation of liquid droplets in saturated vapor, which is responsible for the nucleation. Continuous irradiation pulses maintain the plasma plume formation, which in turn generates a continuous flow of vapor plume increasing the density of formed nucleus. Hugh amount of nuclei favors the growth of nanoparticles, which come in contact and aggregate to form interwoven nanofibrous structure [175].

Also, the anodization was used in order to obtain titania nanofibrous coatings, but only in some very special conditions. Lim and Choi reported that such fibers were obtained on the top of 20 nm in diameter nanotube array, which were more than 10 μm in length [176]. In another report, Chang et al. presented novel method to synthesize nanofibrous coatings—rotating of titanium anode with as-formed nanotube arrays, with the speed of 30 rpm in the same solution, in which the anodization of TNT has taken place (ethylene glycol solution containing 0.3 wt% NH_4F and 2 wt% of H_2O) for next 3 h [177].

Very interesting morphology, from the medical application point of view, has been shown for titania nanofibrous coatings obtained in the process of Ti/Ti alloy chemical oxidation with the use of hydrogen peroxide with or without simple inorganic salts: NaCl, Na_2SO_4, $CaCl_2$, in elevated temperature (80°C) [118].

Wang et al. studied the influence of titania electrospun nanofiber dimensions and microstructure pattern on the adhesion and proliferation of human osteoblasts MG63. Bioactivity of two types of nanofiber dimensions (184 ± 39 nm and 343 ± 98 nm) and two different ways of TNF alignment (flat and patterned TiO_2 nanofibers) were checked and the obtained results indicated that cell morphology was not sensitive to the differences in nanofiber diameter and in microscale structure [178]. These results are in contradiction to some other researchers' studies, which showed preferential cell attachment along patterned TNF. The same authors proved that the combination of microroughness and the nanotopography can be used to modify the differentiation of osteoblasts and generate an osteogenic environment [179–181].

Considering the fact that the rate of osseointegration is strictly related to the efficiency of bone-like apatite formation on the implants, Tavanger et al. used the nanofibers obtained in femtosecond laser ablation process to evaluate the apatite-inducing ability of nanofibrous titania [174]. SEM studies showed that all TNF coatings obtained by Tavanger et al. were covered by dense and homogeneous apatite precipitation layer, after soaking them in simulated body fluid (SBF) for 3 days. EDX results proved that Ca/P ratio was around 1.63, which was attributed to hydroxyapatite, possessing a composition similar to the bone. Moreover, the wettability tests of TNF were performed and very low contact angle (<9.2°), and almost complete spreading of H_2O droplets was observed on all the titania nanofibrous surface samples. Conclusion of the studies was the thesis that TiO_2 nanofibrous structure with the rapid apatite-inducing capability is expected to improve bone formation during *in vivo* implantation [174].

Chang et al. made a bioactivity comparison of different nanomorphology titania coatings: TiO_2 flat, TNT, and TNF, using human osteoblasts MG63. SEM studies revealed that the cell attached to flat TiO_2 possessed a round morphology, whereas these ones attached to nanotubes and nanofibers, showed polygonal shape and extending filopodia. Higher ratio of cell attachment and clearly visible lamellipodia were seen on nanofibrous coatings than on nanotubular ones [177]. This suggests that titania nanofibers surface, because of its rough and porous morphology, provides optimal environment for the cell adhesion, proliferation, and differentiation. The results of bioactivity studies of nanofibrous coatings obtained during Ti/Ti alloy chemical oxidation with the use of hydrogen peroxide with or without simple inorganic salts: NaCl, Na_2SO_4, $CaCl_2$, in elevated temperature (80°C), confirm this [118]. Results of fibroblasts adhesion and proliferation studies carried out with the use of MTT test are shown in **Figure 5**.

Taking into account the different nanotopography and the structure of TNF coatings presented in Ref. [118] (analysis of GAXRD and DRIFT data revealed that TNF obtained in the presence of H_2O_2 and HCl was amorphous with anatase islands; TNF/H_2O_2, TNF/ H_2O_2 + Na_2SO_4, and TNF/ H_2O_2 + NaCl – amorphous with anatase and rutile islands, TNF/ H_2O_2 + $CaCl_2$ – amorphous titania), it can be stated that both above-mentioned attributes influence the bioactivity toward osseointegration processes taking place on their surface.

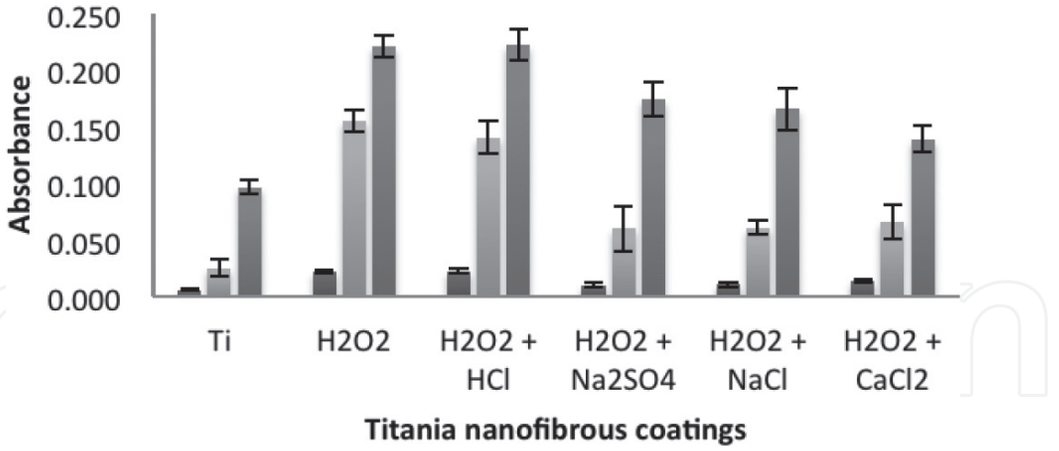

Figure 5. Results of MTT assay carried out on TNF coatings, obtained from different oxidation mixtures, with the use of murine fibroblasts L929 (adhesion after 24 h, proliferation after 72 h and differentiation after 5 days).

Photocatalytic activity of titania nanofibers, obtained by electrospinning method and annealed in 550°C, was studied with the use of dye degradation tests (basic blue 26, basic green 4, basic violet 4) [182]. The concentration of dye solution was measured in relation to UV irradiation time, using UV-Vis spectrophotometer. Additionally, the same tests were done for TiO_2 nanoparticles obtained by sol-gel method and for composite coatings consisting of titania nanofibers and TiO_2 nanoparticles. Doh et al. showed that after 3 h of UV illumination, 25.3% of basic blue 26 was degraded by titania nanofibers. This degradation efficiency was almost the same as for TiO_2 nanoparticles obtained by sol-gel method, for which the value was 23.7%. In comparison, the photoactivity of composite material (TiO_2 nanofibers and TiO_2 nanoparticles) was much higher, as basic blue 26 was degraded by 78.7%. Rate constant calculated for titania nanofibers, titania nanoparticles, and composite material, on the base of simplified equation of the Langmuir-Hinshelwood kinetic model was equal adequately 15.7×10^{-4} min^{-1}, 14.3×10^{-4} min^{-1}, and 85.4×10^{-4} min^{-1}. The values of kinetic rates obtained for composite material but during the degradation processes of dyes: basic green 4 and basic green violet were 81.2×10^{-4} min^{-1} and 67.4×10^{-4} min^{-1}, respectively. Authors concluded that composite materials consisted of TiO_2 nanofibers and TiO_2 nanoparticles had high photocatalytic activity due to their high active surface area and due to complex pore structure. They stated that such materials could be suitable for the application to the degradation of organic dye pollutant.

The photocatalytic activity of TiO_2 nanofibrous coatings obtained during Ti/Ti alloy chemical oxidation with the use of hydrogen peroxide with or without simple inorganic compounds: HCl, NaCl, Na_2SO_4 in 80°C, was analysed also on the base of degradation of two organic pollutant patters: acetone (A) and methylene blue (MB) [118]. Based on the same simplified equation of the Langmuir-Hinshelwood kinetic model, it was possible to calculate the kinetic rates. The values of calculated kinetic rates are showed in **Table 3**.

The values obtained during these studies are very close to those, obtained by Doh et al., however, titania nanofibers obtained in the process of chemical oxidation were not post annealed and they were not enriched by the titania nanoparticles [118, 182]. What should be pointed out clearly is the fact that the observed rate constants do not inform about the real nature of the appropriate processes. However, they provide basic information about change in the

	$10^4\ k_{obs}^{MB}$ (min^{-1})	$10^4\ k_{obs}^{AF}$ (min^{-1})
H_2O_2/Na_2SO_4	81.8 ± 1.0	24.0 ± 0.1
H_2O_2	67.0 ± 3.2	13.5 ± 0.1
H_2O_2/HCl	25.3 ± 0.7	21.3 ± 01
H_2O_2/NaCl	93.6 ± 3.2	14.0 ± 0.1

Table 3. The observed rate constant values for the degradation of MB (k_{obs}^{MB}) and acetone (k_{obs}^{A}) on titania nanofibers under UV light.

degradation rate, depending on the structure, morphology, and active surface of the TiO_2 coatings. The different degradation rate values result from the completely different steps, which occur during the degradation processes: the multistep degradation process of methylene blue (MB) and formation and degradation of some dimeric forms like mesityl oxide, which are observed during acetone degradation.

The results of carried out photocatalytic activity studies showed the potential usefulness of TNF coatings as photoactive ones. Even if they show lower kinetic rate values than titania nanotubes for which these values were almost in all cases five to ten times higher, comparing to titania nanofibers [118].

5. Titania nanowires (TNWs)

From the geometrical point of view, nanowires offer exceptional properties, such as flexibility and fatigue resistance, and the possibility to integrating them in large area with controlled pattern. Sometimes, nanofibers are also used to describe nanowires morphology, especially when nanowires (NW) are very long and not single crystalline. However, in order to achieve 1D NW morphology, it is crucial to obtain one rapid growth direction during the evolution of nanocrystals. This requirement is quite often fulfilled for some crystals, due to the strong anisotropic property of their crystal structures. For example, wurtzite crystals naturally have rapid growth along the [0001] direction and because of this fact NW is one of the preferred morphologies during self-assembly growth. For some other crystals, titania, for example, such anisotrophic behavior is less evident, and they demand additional support to create 1-D nanotopography [159]. Among auxiliary activities, the surface functionalization, introducing dislocations, applying catalysts, and increasing the building block concentration should be mentioned. More detailed strategies for crystal morphology control are given in review articles [182–186]. Plenty of TNW synthesis routes have been examined. Bottom up approaches include a large variety of solution- and vapor-based growth strategies [187–189]. Top down procedures, such as direct oxidation and electrochemical etching techniques, have also been explored for nanowires synthesis [190–192]. The widespread utilization of nanostructured TiO_2, including TNW, is often hindered by the opposite demands for precise control of well-ordered surface features and low-cost rapid production. Taking this into consideration, the synthetic routes, which engaged inexpensive techniques to produce nanowire coatings, are presented in this review.

Most of wet chemical methods require many steps, which increase production costs. Moreover, titania nanostructures, including nanowires, obtained in anodization process or by the electrospinning method, are amorphous, and they need to be annealed in order to endow them in high crystalline form. A method, which can be applied to the formation of titania nanowires, is the thermal oxidation of Ti/Ti alloy surface under a limited supply of oxygen, in argon atmosphere [193–195]. The exposure or pure titanium to argon, which contains ppm of oxygen, at a flow rate of 200 cm^3/min for 8 h at 600°C resulted in the growth of titania nanowires of the length 50–400 nm. Such obtained nanowires posses the structure of rutile. What should be pointed out is the visible impact of the argon flow rate on the morphology of nanostructural TiO_2. Increasing of the flow rate from 200 cm^3/min to 1000 cm^3/min caused the disappearance of nanowires. This effect was even more intensified by the increase of the temperature. Higher flow rate and higher temperature promoted growth of not nanowires but platelets and faceted oxide crystals. It can be concluded that the window of high aspect ratio nanowire growth is very narrow for pure titanium. The situation looks much better in case of titanium alloy—Ti6Al4V. The same procedure of thermal oxidation in the presence of argon both in low and high flow rates gives the same results—titania nanowires. However, the effect of increasing temperature is similar to adequate one for pure titanium. The optimal temperature of the titanium alloy oxidation in order to obtain nanowires is 700°C. At 800°C, a mixture of nanowires and well-faceted crystals is possible to obtain and at 900°C, only platelets and crystals are the results of process. The higher temperature impact on the formation of well-faceted equiaxed crystals indicates that one-dimensional growth at the low temperature is the result of oxidation reaction anisotrophy with the growth preferential on certain crystal faces. At higher temperatures, this anisotrophy decreases and the growth on other surface is promoted, allowing the formation of facetted crystals [194, 195].

My experience with the formation of nanowires, during the titanium direct oxidation, is similar to above mentioned. The use of lower argon flow rate (30 cm^3/min) led to obtain well morphologically oriented nanowires at 475–550°C (**Figure 6a**). Above this temperature, maintaining the same gas flow, facetted crystals were obtained (**Figure 6b**). The addition of H_2O_2 vapors to the carrier gas caused that the formation of nanowires was much slower and less efficient (**Figure 6c**). Prolongation of the process time improved the quality of the nanowires, but only a little, but failed to get a system similar to those received for pure argon (**Figure 6d**).

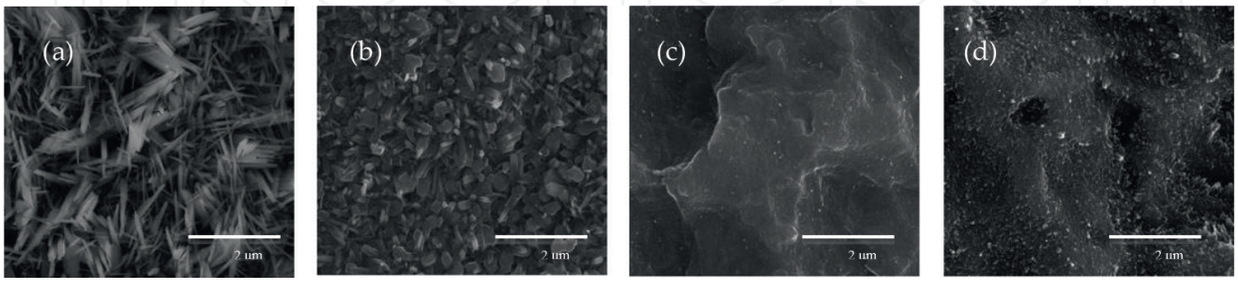

Figure 6. SEM images of titania nanowires obtained in the process of thermal oxidation with the use of pure argon, at 450°C (a), at 600°C (b), and with the use of vapors Ar/H_2O_2, at 500°C, but in 2 h (c) and in 6 h (d).

http://dx.doi.org/10.5772/intechopen.69138

Daothong et al. found that in the presence of adequate organic vapour, titanium can be directly oxidized and TNWs were formed. They presented a size-controlled growth of titania nanowires in the presence of ethanol vapor at high temperature (650–850°C) and low pressure (~10 Torr). The nanowire length was proved to be directly proportional to the oxidation time, and their diameter was strictly connected with applied temperature [196].

The aspect ratio and the shape of titania nanowires were described as resembling the needle-like shape of crystalline hydroxyapatite and collagen fibers found in the bone. Such environment was reported as the place, which ensures the proper cell organization, their vitality, and functionality. Studies on osteoblasts adhesion and growth assessment carried out by Tan et al. showed that osteoblast was able to adhere and spread on the nanowire coating [197]. Osteoblasts adhered to the surface, exhibited an oval shape on the first day and polygonal shape with some protruding lamellipodia on days 3–7. On day 14, osteoblasts formed intercellular network and indicated the cell-to-cell communication, by stretching out their filopodia toward each other. Osteoblasts growth was determined with the use of AlmarBlue assay, and it was proved that osteoblasts were able to proliferate on nanowires coatings. The cell number of osteoblasts on TNW coatings was increased significantly over the level of pure titanium sample. Degree of osteoblasts differentiation was investigated with the use of examination of intracellular ALP (key marker) activity. The test showed that until 7 days, the ALP level was significantly higher than for adequate pure titania coatings. Extracellular matrix mineralization of osteoblasts was evaluated on the base of Alizarin Reds. Also, this assay showed that greater number of discrete mineralized nodules in greater abundance was seen on the nanowire surface.

Our studies on the adhesion and proliferation of fibroblasts show that these processes proceed more efficiently on nanowires, but there are no significant difference between nanowire coatings and pure Ti/Ti alloy (**Figure 7**).

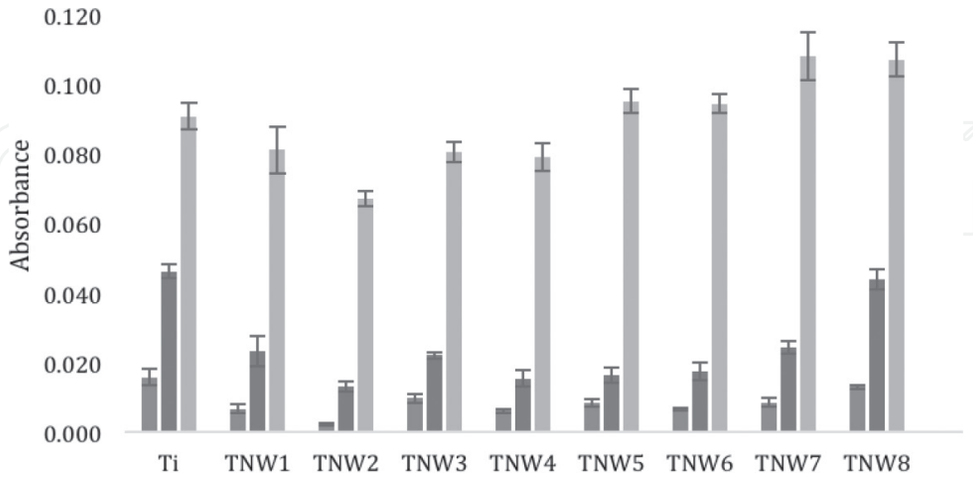

Figure 7. Adhesion (after 24 h) and proliferation (after 72 h and 5 days) of fibroblasts on the surface of titania nanowires obtained at different conditions of temperature and Ar rate flow: TNW1–TNW4 (475°C), TNW5–TNW8 (500°C), TNW1, TNW3, TNW5, TNW7 (30 cm^3/min), TNW2, TNW4, TNW6, TNW8 (100 cm^3/min).

Assuming the biological activity of all reviewed titania nanostructures, it can be stated that at the moment, titania nanotubes are the strongest used in biomedical applications, as the procedure of their fabrication is the most predictable and easy. However, the necessity of their further annealing may lead to the increase of the interest to systems, e.g., TNW, during the production of which, a specific crystalline structure is formed.

The photoactivity of titania nanowires should also be taken into the consideration as such activity gives the possibility to use these coatings in the process of UV-activated sterilization. Most of earlier reports showed the usefulness of titania nanowires rather in the processes of photoelectrochemical water splitting than in the degradation of organic pollutants. In case of sooner, the photoactivity of Au-decorated TiO_2 nanowires electrodes for photoelectrochemical water oxidation, was enhanced in the entire UV-VIS region by the manipulation of the shape of decorated Au nanostructures: nanoparticles and nanorods [198]. The titania nanowires photoactivity in the degradation of 4-chlorophenol was studied by Stengl et al. [199] They calculated the degradation rate constant assuming the reaction kinetic of the first order. The obtained values were in the range 0.0045–0.0083 min^{-1}. So, they were comparable with those obtained for titania nanofibers. The authors noticed that the photocatalytic activity of the annealed samples gradually increased from the temperature of 350°C (0.0045 min^{-1}) to 750°C (0.0129 min^{-1}), and for the samples annealed to temperatures 900°C and 1000°C, respectively, the photoactivity decreased (0.0104 and 0.0083 min^{-1}). They assumed that the initial photocatalytic activity growth for samples annealed in the range 350–750°C corresponds with enlargement of the anatase crystalline phase in consequence of annealing. The decrease of photocatalytic activity of the sample heated above 750°C, they associated this with the transformation of anatase to rutile phase and also with the lowering of surface area. In case of samples obtained in our lab during the thermal oxidation of titanium, in which the rutile phase was present, the calculated rate constants for the methylene blue photodegradation process were in the range 0.0001–0.0002 min^{-1}, so much lower than in case of Ref. [199]. The rutile structure and the low surface area (see **Figure 6c** and **d**) were burdened of such low activity reason.

Author details

Aleksandra Radtke

Address all correspondence to: aradtke@umk.pl

Faculty of Chemistry, Nicolaus Copernicus University in Toruń, Torun, Poland

References

[1] Williams D. On the nature of biomaterials. Biomaterials. 2009;**30**:5897-5909

[2] Mihov D, Katerska B. Some biocompatible materials used in medical practice. Trakia Journal of Sciences. 2010;**8**:119-125

[3] Ratner BD, Hoffman AS, Schoen FJ, Lemons JE, editors. Biomaterials Science—An Introduction to Materials in Medicine. New York; Academic Press, Elsevier; 2013. pp. 37-132

[4] Bhat S, Kumar A. Biomaterials and bioengineering tomorrow's healthcare. Biomatter. 2013;**3**(3):e24717

[5] Bae H, Chu H, Edalat F, Cha JM, Sant S, Kashyap A, Ahari AF, Kwon CH, Nichol JW, Manoucheri S. Development of functional biomaterials with micro-and nanoscale technologies for tissue engineering and drug delivery applications, Journal of Tissue Engineering and Regenerative Medicine. 2014;**8**:1-14

[6] Davis JR. Overview of biomaterials and their use in medical devices. In: Davis JR, editor. Handbook of Materials for Medical Devices. Illustrated edition, Ohio: ASM International; 2003. pp. 1-11

[7] Ramakrishna S, Mayer J, Wintermantel E, Leong KW. Biomedical applications of polymer-composite materials: A review. Composites Science and Technology. 2001;**61**:1189-1224

[8] Williams D. An introduction to medical and dental materials. In: Williams D, editor. Concise Encyclopedia of Medical & Dental Materials. Pergamon Press, Oxford and The MIT Press Cambridge, 1990

[9] Williams D. Titanium in medicine: Material science, surface science. In: Brunette DM, Tengvall P, Textor M, Thompson P, editors. Engineering, Biological Responses and Medical Applications. Berlin and Heidelberg: Springer-Verlag; 2001. pp. 13-24

[10] Geetha M, Singh A, Asokamani R, Gogia A. Ti based biomaterials, the ultimate choice for orthopaedic implants—A review. Progress in Materials Science. 2009;**54**:397-425

[11] Ratner B. Titanium in medicine: Material science, surface science. In: Brunette DM, Tengvall P, Textor M, Thompson P, editors. Engineering, Biological Responses and Medical Applications. Berlin and Heidelberg: Springer-Verlag; 2001. pp. 1-12

[12] Liu X, Chu P, Ding C. Surface modification of titanium, titanium alloys, and related materials for biomedical applications. Materials Science and Engineering R. 2004;**47**:49-121

[13] Adya M, Alam M, Ravindranath T, Mubeen A, Saluja B. Corrosion in titanium dental implants: Literature review. The Journal of Indian Prosthodontic Society. 2005;**5**:126-131

[14] Donachie MJ. Titanium: A Technical Guide. ASM International, Material Park, OH, USA, 2000

[15] Brown S, Lemons J. Medical Applications of Titanium and Its Alloys: The Material and Biological Issues. ASTM special series publication, West Conshohocken, PA, USA. 1272; 1996

[16] Oldani C, Dominguez A. Titanium as a biomaterial for implants. In: Fokter S, editor. Recent Advances in Arthroplasty. InTech, Rijeka, Croatia; 2012. ISBN: 978-953-307-990-5. Available from: http://www.intechopen.com/books/recent-advances-in-arthroplasty/titanium-as-a-biomaterial-for-implants

[17] Van Noort R. Titanium: The implant material for today. Journal of Material Science. 1987;**22**:3801-3811

[18] Bardos DI. Titanium and titanium alloys. In: M'illiams D, editor. Concise Encyclopedia of Medical and Dental Materials. Oxford: Pergamon Press; 1990. pp. 360-365

[19] Sykaras N, Lacopino AM, Marker VA, Triplett RG, Woody RD. Implant materials, designs, and surface topographies: Their effect on osseointegration. A literature review. The International Journal of Oral & Maxillofacial Implants. 2000;**15**:675-690

[20] Adell R, Eriksson B, Lekholm U, Brånemark PI, Jemt T. A long-term follow-up study of osseointegrated implants in the treatment of totally edentulous jaws. International Journal of Oral & Maxillofacial Implants. 1990;**5**:347-359

[21] Niinomi M. Mechanical properties of biomedical titanium alloy. Materials Science and Engineering: A. 1998;**243**:231-236

[22] Branemark R, Branemark PI, Rydevik B, Myers RR. Osseointegration in skeletal reconstruction and rehabilitation: A review. Journal of Rehabilitation Research and Development. 2001;**38**:175-181

[23] Wang W, Poh CK. Titanium alloys in orthopaedics. In: Sieniawski J, editor. Titanium Alloys—Advances in Properties Control. InTech, Rijeka, Croatia; 2013. DOI: 10.5772/55353. Available from: http://www.intechopen.com/books/titanium-alloys-advances-in-properties-control/titanium-alloys-in-orthopaedics

[24] Shah FA, Trobos M, Thomsen P, Palmquist A, Commercially pure titanium (cp-Ti) *versus* titanium alloy (Ti6Al4V) materials as bone anchored implants—Is one truly better than the other? Materials Science and Engineering: C. 2016;**62**:960-966

[25] Wolfle JV, Fiedler J, Durselen L, Reichert J, Scharnweber D, Forster A, Schwenzer B, Reichel H, Ignatius A, Brenner RE. Improved anchorage of Ti6Al4V orthopaedic bone implants through oligonucleotide mediated immobilization of BMP-2 in osteoporotic rats. PLoS One. 2014;**9**:e86151

[26] Ryhänen J, Niemi E, Serlo W, Niemelä E, Sandvik P, Pernu H, Salo T. Biocompatibility of nickel-titanium shape memory metal and its corrosion behavior in human cell cultures. Journal of Biomedical Materials Research. 1997;**35**:451-457

[27] Meisner LL, Markov AB, Proskurovsky DI, Rotshtein VP, Ozur GE, Meisner SN, Yakovlev EV, Poletika TM, Girsova SL, Semin VO. Effect of inclusions on cratering behavior in TiNi shape memory alloys irradiated with a low-energy, high-current electron beam. Surface and Coatings Technology. 2016;**302**:495-506

[28] Mohamed DS, Lotfy KM. Biocompatibility of nickel titanium versus nitrided nickel titanium in bone and bone marrow of male New Zealand rabbits. The Egyptian Journal of Histology. 2015;**38**:629-636

[29] Nasakina EO, Sevost'yanov MA, Gol'dberg MA. Long-term corrosion tests of nanostructural nitinol of (55.91 wt% Ni, 44.03 wt% Ti) composition under static conditions: Ion release, Inorganic Materials: Applied Research. 2015;**6**:59-66

[30] Shabalovskaya S. On the nature of the biocompatibility and medical applications of NiTi shape memory and superelastic alloys. Bio-Medical Materials and Engineering. 1996;**6**:267-289

[31] Sieniawski J, Ziaja W, Kubiak K, Motyka M. Microstructure and mechanical properties of high strength two-phase titanium alloys. In: Sieniawski J, editor. Titanium Alloys—Advances in Properties Control. InTech, Rijeka, Croatia; 2013. DOI: 10.5772/56197. Available from: http://www.intechopen.com/books/titanium-alloys-advances-in-properties-control/microstructure-and-mechanical-properties-of-high-strength-two-phase-titanium-alloys

[32] Hosseini S, Limooei MB. Investigation of fatigue behavior and notch sensitivity of Ti-6Al-4V. Applied Mechanics and Materials. 2001;**7**:80-81

[33] Hosseini S, Arabi H, Tamizifar M, Zeyaei A. Effect of tensile strength on behavior and notch sensitivity of Ti-6Al-4V. Iranian Journal of Materials Science and Engineering. Vol. 3. Winter & Spring; 2006. pp. 12-16

[34] Steinemann SG. Corrosion of Titanium and Titanium Alloys for Surgical Implants, Titanium 84 Science and Technology. Vol.2, Deutsche Gesellschaft Fur Metallkunde EV, Munich, Germany: 1985. pp. 1373-1379

[35] Hiromoto S, Hanawa T, Asami K. Composition of surface oxide film of titanium with culturing murine fibroblasts L929. Biomaterials. 2004;**25**:979-986

[36] Hanawa T, Asami K, Asaoka K. Repassivation of titanium and surface oxide film regenerated in simulated bioliquid. Journal of Biomedical Materials Research. 1998;**40**:530-538

[37] Nasakina EO, Sevost'yanov MA, Gol'dberg MA, Demin KY, Baikin AS, Goncharenko BA, Cherkasov VA, Kolmakov AG, Zabolotnyi VT. Long-term corrosion tests of nanostructural nitinol of (55.91 wt% Ni, 44.03 wt% Ti) composition under static conditions: Composition and structure before and after corrosion. Inorganic Materials: Applied Research. 2015;**6**:59-66

[38] Le Gué hennec L, Soueidan A, Layrolle P, Amouriq Y. Surface treatments of titanium dental implants for rapid osseointegration. Dental Materials. 2007;**23**:844-854

[39] Carlsson L, Röstlund T, Albrektsson B, Albrektsson T, Brånemark P-I. Osseointegration of titanium implants. Acta Orthopaedica Scandinavica. 1986;**57**:285-289

[40] Elias CN, Meirelles L. Improving osseointegration of dental implants. Expert Review of Medical Devices. 2010;**7**:241-256

[41] Hao J, Li Y, Li B, Wang X, Li H, Liu S, Liang C, Wang H. Biological and mechanical effects of micro-nanostructured titanium surface on an osteoblastic cell line in vitro and osteointegration in vivo. Applied Biochemistry and Biotechnology. 2017 Mar 20. DOI: 10.1007/s12010-017-2444-1

[42] Branemark P, Hansson B, Adell R, Breine U, Lindstrom J, Hallen O, Ohman A. Osseointegrated implants in the treatment of edentulous jaw. Scandinavian Journal of Plastic and Reconstructive Surgery Supplement. 1977;**16**:1-132

[43] Coathup MJ, Blunn GW, Mirhosseini N, Erskine K, Liu Z, Garrod DR, Li L. Controlled laser texturing of titanium results in reliable osteointegration. Journal of Orthopaedic Research. 2016 Jun 16. DOI: 10.1002/jor.23340

[44] Mavrogenis AF, Dimitriou R, Parvizi J, Babis GC. Biology of implant osseointegration. Journal of Musculoskeletal and Neuronal Interactions. 2009;**9**:61-71

[45] Schatzker J. Osseointegration of metal. Canadian Journal of Surgery. 1995;**38**:49-54

[46] Wróbel E, Witkowska-Zimny M, Przybylski J. Biological mechanisms of implant osseointegration. Ortopedia Traumatologia Rehabilitacja. 2010;**12**:401-409

[47] Junker R, Dimakis A, Thoneick M, Jansen JA. Effects of implant surface coatings and composition on bone integration: A systematic review Clinical Oral Implants Research. 2009;**4**:185-206

[48] Molitor P, Barron V, Young T. Surface treatment of titanium for adhesive and adhesives. International Journal of Adhesion and Adhesives. 2001;**21**(2):129-136

[49] Citeau A, Guicheux J, Vinatier C, Layrolle P, Nguyen TP, Pilet P, Daculsi G. In vitro biological effects of titanium rough surface obtained by calcium phosphate grid blasting. Biomaterials. 2005;**26**:157-165

[50] Liang CY, Yang XJ, Wei Q, Cui ZD. Comparison of calcium phosphate coatings formed on femtosecond laser-induced and sand-blasted titanium. Applied Surface Science. 2008;**255**:515-518

[51] Gbureck U, Masten A, Probst J, Thull R. Tribochemical structuring and coating of implant metal surfaces with titanium oxide and hydroxyapatite layers. Materials Science and Engineering C. 2003;**23**:461-465

[52] Hryniewicz T, Rokicki R, Rokosz K. Corrosion and surface characterization of titanium biomaterial after magnetoelectropolishing. Surface & Coatings Technology. 2009;**203**:1508-1515

[53] Strnad J, Strnad Z, Sestak J. Physico-chemical properties and healing capacity of potentially bioactive titanium surface. Journal of Thermal Analysis and Calorimetry. 2007;**88**(3):775-779

[54] Mohammadi Z, Ziaei-Moayyed AA, Sheikh-Mehdi Mesgar A. Grit blasting of Ti-6Al-4V alloy: Optimization and its effect on adhesion strength of plasma-sprayed hydroxyapatite coatings. Journal of Materials Processing Technology. 2007;**194**:15-23

[55] Lu X, Zhao Z, Leng Y. Biomimetic calcium phosphate coatings on nitric-acid-treated titanium surfaces. Materials Science and Engineering C. 2007;**27**:700-708

[56] Yousefpour M, Afshar A, Chen J, Xingdong Z. Bioactive layer formation on alkaline-acid treated titanium in simulated body fluid. Materials and Design. 2007;**28**:2154-2159

[57] Pattanayak DK, Kawai T, Matsushita T, Takadama H, Nakamura T, Kokubo T. Effect of HCl concentrations on apatie-forming ability of NaOH-HCl- and heat-treated titanium metal. Journal of Materials Science: Materials in Medicine. 2009;**20**:2401-2411. http://www.springerlink.com/content/m7l108m885m83056

[58] Assis SL, Costa I. The effect of hydrogen peroxide on the electrochemical behaviour of Ti-13Nb-13Zr alloy in hanks' solution. Materials Research. 2006;**9**(4):425-429

[59] Han JY, Zu ZT, Zhou L. Hydroxyapatite/titania composite bioactivity coating processed by sol-gel method. Applied Surface Science. 2008;**255**:455-458

[60] Nguyen HQ, Deporter DA, Pilliar RM, Valiquette N, Yakubovich R. The effect of sol-gel formed calcium phosphate coatings on bone ingrowth and osteoconductivity of porous-surfaced Ti alloy implants. Biomaterials. 2004;**25**(5):865-876

[61] Wierzchon T, Czarnowska E, Krupa D. Inżynieria powierzchni w wytwarzaniu biomateriałów tytanowych. Warszawa: Oficyna Wyd. Politechniki Warszawskiej; 2004

[62] Wilks RG, Santos E, Kurmaev EZ, Yablonskikh MV, Moewes A, Kuromoto NK, Soares GA. Characterization of oxide layers fordem on electrochemically treated Ti by Rusing soft X-ray absorption measurements. Journal of Electron Spectroscopy and Related Phenomena. 2009;**169**:46-50

[63] Diamanti MV, Pedeferri MP. Effect of anodic oxidation parameters on the titanium oxides formation. Corrosion Science. 2007;**49**:939-948

[64] Cui X, Kim H-M, Kawashita M, Wang L, Xiong T, Kokubo T, Nakamura T. Preparation of bioactive titania films on titanium metal via anodic oxidation. Dental Materials. 2009;**25**:80-86

[65] Bauer S, Park J, Mark K, Schmuki P. Improved attachment of mesenchymal stem cells on super-hydrophobic TiO_2 nanotubes. Acta Biomaterialia. 2008;**4**:576-1582

[66] Goto T. Surface coating technology for biomaterials—morphology and nono-structure control. International Congress Series. 2005;**1284**:248-256

[67] Sevilla P, Aparicio C, Planell JA, Gil FJ. Comparison of the mechanical properties between tantalum and nickel-titanium foams implant materials for bone ingrowth applications. Journal of Alloys and Compounds. 2007;**439**:67-73

[68] Trommer RM, Santos LA, Bergmann CP. Alternative technique for hydroxyapatite coatings. Surface & Coatings Technology. 2007;**201**:9587-9593

[69] Kim DS, Han SJ, Kwak S-Y. Synthesis and photocatalytic activity of mesoporous TiO_2 with the surface area, crystallite size, and pore size. Journal of Colloid and Interface Science. 2007;**316**:85-91

[70] Baram N, Starosvetsky D, Starosvetsky J, Epshtein M, Armon R, Ein-Eli Y. Enhanced inactivation of *E. coli* bacteria using immobilized porous TiO_2 photoelectrocatalysis. Electrochimica Acta. 2009;**54**:3381-3386

[71] Lewis G, McVay B. Effect of thermal spray process for deposition hydroxyapatite coating on a titanium alloy on its fatigue performance. Proceedings of the 17th Southern Biomedical Engineering Conference 1998, p.119

[72] Gledhill HC, Turner IG, Doyle C. In vitro dissolution behavior of two morphologically different thermally sprayed hydroxyapatite coatings. Biomaterials. 2001;**22**:695-700

[73] Li H, Khor KA. Characteristics of the nanostructures in thermal sprayed hydroxyapatite coatings and their influence on coating properties. Surface & Coatings Technology. 2006;**201**:2147-2154

[74] Lima RS, Khor KA, Li H, Cheang P, Marple BR. HVOF spraying on nanostructured hydroxyapatite for biomedical applications. Materials Science and Engineering A. 2005;**396**:181-187

[75] Goana M, Lima RS, Marple BR. Influence of particle temperature and velocity on the microstructure and mechanical behavior of high velocity oxy-fuel (HVOF)—sprayed nanostructured titania coatings. Journal of Materials Processing Technology. 2008;**198**:426-435

[76] Hoseini M, Jedenmalm A, Boldizar A. Tribological investigation of coatings for artificial joints. Wear. 2008;**264**:958-966

[77] Chiu S-M, Chen Z-S, Yang K-Y, Hsu Y-L, Gan D. Photocatalytic activity of moped TiO2 coatings prepared by sputtering deposition. Journal of Materials Processing Technology. 2007;**192-193:**60-67

[78] Krupa D, Baszkiewicz J, Rajchel B, Barcz A, Sobczak JW, Biliński A, Borowski T. Effect of calcium-ion implantation on the corrosion resistance and bioactivity of the Ti6Al4V Allom. Vacuum. 2007;**81**:1310-131

[79] Xie Y, Liu X, Huang A, Ding CH, Chu PK. Improvement of surface bioactivity on titanium by water and hydrogen plasma immersion ion implantation. Biomaterials. 2005;**26**:6129-6135

[80] Jo YJ, Lee CM, Jang HS, Lee NS, Suk J-H, Lee WH. Mechanical properties of fully porous and porous-surfaced Ti-6Al-4V implants fabricated by electro-discharge-sintering. Journal of Materials Processing Technology. 2007;**194**:121-125

[81] An YB, Lee WH. Synthesis of porous titanium implants by environmental- electro-discharge-sintering process. Materials Chemistry and Physics. 2006;**95**:242-247

[82] Hanaor DAH, Sorrell CHC. Review of the anatase to rutile phase transformation. Journal of Materials Science. 2011;**46**:855-874

[83] Gateshki M, Yin S, Ren Y, Petkov V. Titania polymorphs by soft chemistry: Is there a common structural pattern? Chemistry of Materials. 2007;**19**:2512-2518

[84] Diebold U. Structure and properties of TiO_2 surfaces: A brief review. Applied Physics A. 2003;**76**:681-687

[85] Wang B, Qi H, Wang H, Cui Y, Zhao J, Guo J, Cui Y, Liu Y, Yi K, Shao J. Morphology, structure and optical properties in TiO2 nanostructured films annealed at various temperatures. Optical Materials Express. 2015;**5**:1410-1418

[86] Park J-Y, Lee CH, Jung K-W, Jung D. Structure related photocatalytic properties of TiO_2. Bulletin of the Korean Chemical Society. 2009;**30**:402-404

[87] Alemany LJ, Bañares MA, Pardo E, Martín-Jiménez F, Blasco JM. Morphological and structural characterization of a titanium dioxide system. Materials Characterization. 2000;**44**:271-275

[88] Thamaphat K, Limsuwan P Ngotawornchai B. Phase Characterization of TiO2 Powder by XRD and TEM. Kasetsart Journal (Natural Science) 2008;**42**:357-361

[89] Sakurai K, Mizusawa M. X-ray diffraction imaging of anatase and rutile. Analytical Chemistry. 2010;**82**:3519-3522

[90] Thangavelu K, Annamalai R, Arulnandhi D. Synthesis and characterization of nanosized TiO_2 powder derived from a sol-gel process in acidic conditions. International Journal of Engineering Sciences & Emerging Technologies. 2013;**4**:90-95

[91] Rao CNR, Turner A, Honig JM. The effect of impurities on the anatase-rutile transformation. The Journal of Physical Chemistry. 1959;**11**:173-174

[92] Oshaka T, Izumi F, Fujiki Y. Raman spectrum of anatase TiO_2. Journal of Raman Spectroscopy. 1978;**7**:321-324

[93] Deo G, Turek AM, Wachs IE, Machej T, Haber J, Das N, Edkert H, Hirt AM. Physical and chemical characterization of surface vanadium-oxide supported on titania. Influence of the titania phase (anatase, rutile, brookite A and B). Applied Catalysis A. 1992;**A91**:27-42

[94] Alemany LJ, Bañares MA, Larrubia MA, Jiménez MC, Delgado F, Blasco JM. Vanadia-titania systems—Morphological and structural properties. Materials Research Bulletin. 1996;**31**:513-520

[95] Zeng G, Li K-K, Yang H-G, Zhang Y-H. Micro-Raman mapping on an anatase TiO_2 single crystal with a large percentage of reactive (0 0 1) facets. Vibrational Spectroscopy. 2013;**68**:279-284

[96] Foucher F, Guimbretière G, Bost N, Westall F. Petrographical and Mineralogical applications of Raman mapping. In: Maaz K, editor. Raman Spectroscopy and Applications. InTech, Rijeka, Croatia; 2017. ISBN 978-953-51-2908-0, Print ISBN 978-953-51-2907-3

[97] Jianliang LJ, BoWang B, Sproul WD, Ou Y, Dahan I. Anatase and rutile TiO_2 films deposited by arc-free deep oscillation magnetron sputtering. Journal of Physics D: Applied Physics. 2013;**46**:084008 (9 pp)

[98] Dai S, Wu Y, Sakai T, Du Z, Sakai H, Abe M. Preparation of highly crystalline TiO_2 nanostructures by Acid-assisted hydrothermal treatment of Hexagonal-structured nanocrystalline titania/cetyltrimethyammonium bromide nanoskeleton. Nanoscale Researh Letter. 2010;**11:**1829-1835

[99] Roy P, Berger S, Schmuki P. TiO_2 Nanotubes: Synthesis and applications. Angewandte Chemie International Edition. 2011;**50**:2904-2939

[100] Regonini D, Bowen CR, Jaroenworaluck A, Stevens R. A review of growth mechanism, structure and crystallinity of anodized TiO_2 nanotubes. Materials Science and Engineering: R: Reports. 2013;**74**:377-406

[101] Wang Y, Wu Y, Qin Y, Xu G, Hu X, Cui J, Zheng H, Hong Y, Zhang X. Rapid anodic oxidation of highly ordered TiO_2 nanotube arrays. Journal of Alloys and Compounds. 2011;**509**:157-160

[102] Zhao J, Wang X, Chen R, Li L. Fabrication of titanium oxide nanotube arrays by anodic oxidation. Solid State Communications. 2005;**134**:705-710

[103] Sulka GD, Kapusta-Kołodziej J, Brzózka A, Jaskuła M. Anodic growth of TiO_2 nanopore arrays at various temperatures. Electrochimica Acta. 2013;**104**:526-535

[104] Diamanti MV, Spreafico FC, Pedeferri MP. Production of anodic TiO_2 nanofilms and their characterization. Physics Procedia. 2013;**40**:30-37

[105] Komiya S, Sakamoto K, Ohtsu N. Structural changes of anodic layer on titanium in sulfate solution as a function of anodization duration in constant current mode. Surface Science. 2014;**296**:163-168

[106] Kuromoto NK, Simão RA, Soares GA. Titanium oxide films produced on commercially pure titanium by anodic oxidation with different voltages. Materials Characterization. 2007;**58**:114-121

[107] Kasuga T, Hiramatsu M, Hoson A, Sekino T, Niihara K. Formation of titanium oxide nanotube. Langmuir. 1998;**14**:3160-3163

[108] Sander MS, Cote MJ., Gu W, Kile BM, Tripp CP. Template-Assisted fabrication of dense, aligned arrays of titania nanotubes with Well-Controlled dimensions on substrates. Advanced Materials. 2004;**16**:2052-2057

[109] Adachi M, Murata Y, Harada M, Yoshikawa S. Formation of titania nanotubes with high photo-catalytic activity. Chemical Letters. 2000;**29**:942-943

[110] Lakshmi BB, Dorhout PK, Martin CR. Sol-gel template synthesis of semi-conductor nanostructures. Chemistry of Materials. 1997;**9**:857-862

[111] Kasuga T, Hiramatsu M, Hoson A, Sekino T, Niihara K. Titania nanotubes prepared by chemical processing. Advanced Materials. 1999;**11**:1307-1311

[112] Kulkarni M, Mazare A, Schmuki P, Iglic A. Influence of anodization parameters on morphology of TiO_2 nanostructured surfaces. Advanced Materials Letters. 2016;**7**:23-28

[113] Lim Y-Ch, Zulkarnain Zainal Z, Wee-Tee Tan W-T, Hussein MZ. Anodization parameters influencing the growth of titania nanotubes and their photoelectrochemical response. International Journal of Photoenergy.2012;**2012**. 9. Article ID 638017. DOI: 10.1155/2012/638017

[114] Haring A, Morris A, Hu M. Controlling morphological parameters of anodized titania nanotubes for optimized solar energy applications. Materials. 2012;5:1890-1909

[115] Amin Yavari S, Chai YC, Böttger AJ, Wauthle R Schrooten J, Weinans H, Zadpoor AA. Effects of anodizing parameters and heat treatment on nanotopographical features, bioactivity, and cell culture response of additively manufactured porous titanium. Materials Science and Engineering C: Materials for Biological Applications. 2015;**51**:132-138

[116] Kaczmarek A, Klekiel T, Krasicka-Cydzik E. Fluoride concentration effect on the anodic growth of self-aligned oxide nanotube array on Ti6Al7Nb alloy. Surface and Interface Analysis. 2010;**42**:510-514

[117] Habazaki H, Fushimi K, Shimizu K, Skeldon P, Thompson GE. Fast migration of fluoride ions in growing anodic titanium oxide. Electrochemistry Communications. 2007;**9**:1222-1227

[118] Radtke A, Piszczek P, Topolski A, Lewandowska Ż, Talik E, Andersen IH, Nielsen LP, Heikkilä M, Leskelä M. The structure and the photocatalytic activity of titania based nanotube and nanofiber coatings. Applied Surface Science. 2016;**368**:165-172

[119] Lee K, Mazare A, Schmuki P. One-Dimensional titanium dioxide nanomaterials: Nanotubes. Chemical Reviews. 2014;**19**:9385-9454

[120] Albu SP, Kim D, Schmuki P. Growth of aligned TiO_2 bamboo-type nanotubes and highly ordered nanolace. Angewandte Chemie International Edition. 2008;**47**:1916-1919

[121] Kim D, Ghicov A, Albu SP, Schmuki P. TiO_2 bamboo-type nanotubes: Improved conversion efficiency in dye–sentisized solar cells. Journal of the American Chemical Society. 2008;**130**:16454-16455

[122] Ruan CH, Paulose M, Varghese OK, Mor GK, Grimes CA. Fabrication of highly ordered TiO_2 nanotube arrays using an organic electrolyte. Journal of Physical Chemistry B. 2005;**109**:15754-15759

[123] Yoriya S, Mor GK, Sharma S, Grimes CA. Synthesis of ordered arrays of discrete, partially crystalline titania nanotubes by Ti anodization using diethylene glycol electrolytes. Journal of Materials Chemistry. 2008;**18**:3332-3336

[124] Yoriya S, Grimes CA. Self-assembled TiO_2 nanotube arrays by anodization of titanium in diethylene glycol: Approach to extended pore widening. Langmuir. 2010;**26**(1):417-420

[125] Hassan FMB, Nanjo H, Tetsuka H, Kanakubo M, Aizawa T, Nishioka M, Ebina T. Formation of self ordered TiO_2 nanotubes by electrochemical anodization of titanium in 2-Propanol/NH4F. ECS Transactions. 2009;**16**:35-47

[126] Xiong JY, Wang Y, An Y, Wen M, Ding YF, Li YC, Hodgson P. Morphology evolution during annealing and electrical conductivity of titania nanotube films. Advanced Materials Research. 2012;**399-401**:548-551

[127] Bayram C, Demirbilek M, Calişkan N, Demirbilek ME, Denkbaş EB. Osteoblast activity on anodized titania nanotubes: Effect of simulated body fluid soaking time. Journal of Biomedical Nanotechnology. 2012;**8**:482-490

[128] Minagar S, Wang J, Berndt CC, Ivanova EP, Wen C. Cell response of anodized nanotubes on titanium and titanium alloys. Journal of Biomedical Materials Research Part A. 2013;**101**:2726-2739

[129] Gongadze E, Kabaso D, Bauer S, Park J, Schmuki P, Iglič A. Adhesion of osteoblasts to a vertically aligned TiO_2 nanotube surface. Mini Reviews in Medicinal Chemistry. 2013;**13**:194-200

[130] Tan AW, Pingguan-Murphy B, Ahmad R, Akbar SA. Review of titania nanotubes: Fabrication and cellular response. Ceramics International. 2012;**38**:4421-4435

[131] Smith BS, Yoriya S, Johnson T, Popat KC. Dermal fibroblast and epidermal keratinocyte functionality on titania nanotube arrays. Acta Biomaterialia. 2011;**7:**2686-2696

[132] Bariana M, Dwivedi P, Ranjitkar S, Kaidonis JA, Losic D, Anderson PJ. Biological response of human suture mesenchymal cells to titania nanotube-based implants for advanced craniosynostosis therapy. Colloids and Surfaces B: Biointerfaces. 2017;**1**:59-67

[133] Burns K, Yao C, Webster TJ. Increased chondrocyte adhesion on nanotubular anodized titanium. Journal of Biomedical Materials Research Part A. 2009;**88A**:561-568

[134] Park J, Bauer S, Schlegel KA, Neukam FW, von der Mark K, Schmuki P. TiO_2 nanotube surfaces: 15 nm—an optimal length scale of surface topography for cell adhesion and differentiation. Small. 2009;**5**:666-671

[135] Park J, Bauer S, von der Mark K, Schmuki P. Nanosize and vitality: TiO_2 nanotube diameter directs cell fate. Nano Letters. 2007;**7**(6):1686-1691

[136] Lewandowska Ż, Piszczek P, Radtke A, Jędrzejewski T, Kozak W, Sadowska B. The evaluation of the impact of titania nanotube covers morphology and crystal phase on their biological properties. Journal of Materials Science: Materials in Medicine. 2015;**26**:163

[137] Ercan B, Taylor E, Alpaslan E, Webster T. Diameter of titanium nanotubes influences anti-bacterial efficacy. Journal of Nanotechnology. 2011;**22**:295102

[138] Ercan B, Kummer KM, Tarquinio KM, Webster TJ. Decreased *Staphylococcus aureus* biofilm growth on anodized nanotubular titanium and the effect of electrical stimulation. Acta Biomaterialia. 2011;**7**:3003-3012

[139] Popat KC, Eltgroth M, Latempa TJ, Grimes CA, Desai TA. Decreased *Staphylococcus epidermis* adhesion and increased osteoblast functionality on antibiotic-loaded titania nanotubes. Biomaterials. 2007;**28**:4880-4888

[140] Cipriano AF, Miller C, Liu H. Anodic growth and biomedical applications of TiO_2 nanotubes. Journal of Biomedical Nanotechnology. 2014;**10**:2977-3003

[141] Puckett DS, Tayler E, Raimondo T, Webster TJ. The relationship between the nanostructure of titanium surfaces and bacterial attachment. Biomaterials. 2010;**31**:706-713

[142] Akira Fujishima A, Rao TN, Tryk DA. Titanium dioxide photocatalysis. Journal of Photochemistry and Photobiology C: Photochemistry Reviews. 2000;**1**:1-21

[143] Diebold U. The surface science of titanium dioxide. Surface Science Reports. 2003;**48**:53-229

[144] Carp O, Huisman CL, Reller A. Photoinduced reactivity of titanium dioxide. Progress in Solid State Chemistry. 2004;**32**:33-177

[145] Fujishima A, Zhang X, Tryk DA. TiO_2 photocatalysis and related surface phenomena. Surface Science Reports. 2008;**63**:515-582

[146] Schneider J, Matsuoka M, Takeuchi M, Zhang J, Horiuchi Y, Anpo M, Bahnemann DW. Understanding TiO_2 photocatalysis: Mechanisms and materials. Chemical Reviews. 2014;**114**:9919-9986

[147] Paz Y. Application of TiO_2 photocatalysis for air treatment: Patents' overview. Review Article. Applied Catalysis B: Environmental. 2010;**99**(3-4):448-460

[148] Pelaez M, Nolan NT, Pillai SC, Seery MK, Falaras P, Kontos AG, Dunlop P, Hamilton J, Byrne JA, O'Shea K, Entezari MH., Dionysiou D. A review on the visible light active titanium dioxide photocatalysts for environmental applications. Applied Catalysis B: Environmental. 2012;**125**:331-349

[149] Park H, Park Y, Kim W, Choi W. Surface modification of TiO_2 photocatalyst for environmental applications. Journal of Photochemistry and Photobiology C: Photochemistry Reviews. 2013;**15**:1-20

[150] Herrmann J-M. Fundamentals and misconceptions in photocatalysis. Journal of Photochemistry and Photobiology A: Chemistry. 2010;**216**:85-93

[151] Feng T, Feng GS, Yan L, Pan JH. One-Dimensional nanostructured TiO_2 for photocatalytic degradation of organic pollutants in wastewater. International Journal of Photoenergy. 2014;**14**. Article ID 563879

[152] Albu SP, Ghicov A, Macak JM, Hahn R, Schmuki P. Self-organized, free-standing TiO_2 nanotube membrane for flow-through photocatalytic applications Nano Letters. 2007;**7**:1286-1289

[153] Macak JM, Zlamal M, Krysa J, Schmuki P. Self-organized TiO_2 nanotube layers as highly efficient photocatalysts. Small. 2007;**3**:300-304

[154] Lee K, Mazare A, Schmuki P. One-dimensional titanium dioxide nanomaterials: Nanotubes. Chemical Reviews. 2014;**114**:9385-9454

[155] Paramasivam I, Macak JM, Ghicov A, Schmuki P. Enhanced photochromism of Ag loaded self-organized TiO_2 nanotube layers. Chemical Physics Letters. 2007;**445**:233-237

[156] Zlamal M, Macak JM, Schmuki P, Krysa J. Electrochemically assisted photocatalysis on self-organized TiO_2 nanotubes. Electrochemistry Communications. 2007;**9**:2822-2826

[157] Paramasivam I, Jha H, Liu N, Schmuki P, A Review of Photocatalysis using Self-organized TiO2 Nanotubes and Other Ordered Oxide Nanostructures, Small 2012;**8**: 3073-3103

[158] Teo WE, Ramakrishna S. A review on electrospinning design and nanofibre assemblies. Nanotechnology. 2006;**17**:89-106

[159] Thoppey NM, Bochinski JR, Clarke LI, Gorga RE. Edge electrospinning for high throughput production of quality nanofibers, Nanotechnology. 2011;**22**. Article ID 345301

[160] Panda PK, Ramakrishna S. Electrospinning of alumina nanofibers using different precursors. Journal of Materials Science. 2007;**42**:2189-2193

[161] Ramaseshan R, Sundarrajan S, Jose R, Ramakrishna S. Nanostructured ceramics by electrospinning. Journal of Applied Physics. 2007;**102**. Article ID 111101

[162] Watthanaarun J, Pavarajarn V, Supaphol P. Titanium(IV) oxide nanofibers by combined sol-gel and electrospinning techniques: Preliminary report on effects of preparation conditions and secondary metal dopant. Science and Technology of Advanced Materials. 2005;**6**:240-245

[163] Chronakis IS. Novel nanocomposites and nanoceramics based on polymer nanofibers using electrospinning process—A review. Journal of Materials Processing Technology. 2005;**167**:283-293

[164] Caratão B, Carneiro E, Sá P, Almeida B, Carvalho S. Properties of Electrospun TiO_2 nanofibers. Journal of Nanotechnology. 2014;**5**. Article ID 472132

[165] Li D, Xia Y. Fabrication of titania nanofibers by electrospinning. Nano Letters. 2003;**3**: 555-560

[166] Lee J-S, Lee Y-I, Song H, Jang D-H, Choa Y-H. Synthesis and characterization of TiO_2 nanowires with controlled porosity and microstructure using electrospinning method. Current Applied Physics. 2011;**11**:210-214

[167] Wang X, Zhu J, Yin L, Liu S, Zhang X, Ao Y, Chen H, Evaluation of the Morphology and Osteogenic Potential of Titania-Based Electrospun Nanofibers, Journal of Nanomaterials, 2012; **2012**:7. Article ID 959578, DOI:10.1155/2012/959578

[168] Ding B, Kim CK, Kim HY, Se MK, Park SJ. Titanium dioxide nanofibers prepared by using electrospinning method. Fibers and Polymers. 2004;**5**:105-109

[169] Chen J-Y, Chen H-C, Lin J-N, Kuo C. Effects of polymer media on electrospun mesoporous titania nanofibers. Materials Chemistry and Physics. 2008;**107**:480-487

[170] Lee S-J, Cho N-I, Lee DY. Effect of collector grounding on directionality of electrospun titania fibers. Journal of the European Ceramic Society. 2007;**27**:3651-3654

[171] Chandrasekar R, Zhang LF, Howe JY, Hedin NE, Zhang Y, Fong H. Fabrication and characterization of electrospun titania nanofibers. Journal of Materials Science. 2009;**44**:1198-1205

[172] Khalil KA, Kim SW, Kim KW, Dharmaraj N, Kim HY. A novel bio-nanocomposites composed of hydroxyapatite reinforced with TiO_2 electrospun nanofiber consolidated using high-frequency induction heating. International Journal of Applied Ceramic Technology. 2011;**8**:523-531

[173] Park S-J, Chase G, Jeong K-U, Kim H. Mechanical properties of titania nanofiber mats fabricated by electrospinning of sol-gel precursor. Journal of Sol-Gel Science and Technology. 2010;**54**:188-194

[174] Tavangar A, Tan B, Venkatakrishnan K. Synthesis of bio-functionalized three dimensional titania nanofibrous structures using femtosecond laser ablation. Acta Biomaterialia. 2011;**7**:2726-2732

[175] Tavangar A, Tan B, Venkatakrishnan K. Study of the formation of 3-D titania nanofibrous structure by MHz femtosecond laser in ambient air. Journal of Applied Physics. 2013;**113**:023102-023110

[176] Lim JH, Choi J. Titanium oxide nanowires originating from anodically grown nanotubes: The bamboo-splitting model. Small. 2007;**3**:1504-1507

[177] Chang CH, Lee HC, Chen CC, Wu Y-H, Hsu Y-M, Chang Y-P, Yang T-I, Fang H-W.A novel rotating electrochemically anodizing process to fabricate titanium oxide surface nanostructures enhancing the bioactivity of osteoblastic cells. Journal of Biomedical Materials Research Part A. 2012;**100A**:1687-1695

[178] Wang X, Gittens RA, Song R, Tannenbaum R, Olivares-Navarrete R, Schwartz Z, Chen H, Boyan BD. Effects of structural properties of electrospun TiO_2 nanofiber meshes on their osteogenic potential. Acta Biomaterialia. 2012;**8**:878-885

[179] Ma JY, He XZ, Jabbari E. Osteogenic differentiation of marrow stromal cells on random and aligned electrospun poly(l-lactide) nanofibers. Annals of Biomedical Engineering. 2011;**39**:14-25

[180] Menel AJ, Kubow KE, Klotzsch E, Garcia-Fuentes M, Smith ML, Vogel V. Optimization strategies for electrospun silk fibroin tissue engineering scaffolds. Biomaterials. 2009;**30**:3058-3067

[181] Murugan R, Ramakrishna S. Design strategies of tissue engineering scaffolds with controlled fiber orientation. Tissue Engineering. 2007;**13**:1845-1866

[182] Doh SJ, Kim CH, Lee SG, Lee SJ, Kim H. Development of photocatalytic TiO_2 nanofibers by electrospinning and its application to degradation of dye pollutants. Journal of Hazardous Materials. 2008;**134**:118-127

[183] Jun Y-W, Choi J-S, Cheon J. Shape control of semiconductor and metal oxide nanocrystals through nonhydrolytic colloidal routes. Angewandte Chemie International Edition. 2006;**45**:3414-3439

[184] Jun Y-W, Lee J-H, Choi J-S, Cheon J. Symmetry-controlled colloidal nanocrystals: Nonhydrolytic chemical synthesis and shape determining parameters. Journal of Physical Chemistry B. 2005;**109**:14795-14806

[185] Niederberger M. Nonaqueous sol-gel routes to metal oxide nanoparticles. Accounts of Chemical Research. 2007;**40**:793-800

[186] Cozzoli PD, Pellegrino T, Manna L. Synthesis, properties and perspectives of hybrid nanocrystal structures. Chemical Society Reviews. 2006;**35**:1195-1205

[187] Lee JC, Park KS, Kim TG, Choi HJ, Sung YM. Controlled growth of high-quality TiO_2 nanowires on sapphire and silica. Nanotechnology. 2006;**17**:4317-4321

[188] Ma R, Fakuda K, Sasaki T, Osada M, Bando Y. Structural features of titanate nanotubes/nanobelts revealed by Raman, X-ray absorption fine structure and electron diffraction characterizations. Journal of Physical Chemistry B. 2005;**109**:6210-6214

[189] Amin SS, Nicholls AW, Xu TT. A facile approach to synthesize single crystalline rutile TiO_2 one-dimensional nanostructures. Nanotechnology. 2007;**18**:445609

[190] Mukherjee K, Teng TH, Jose R, Ramakrishna S. Electron transport in electrospun TiO_2 nanofiber dye-sensitized solar cells. Applied Physics Letters. 2009;**95**:012101

[191] Fujihara K, Kumar A, Jose R, Ramakrishna S. Spray deposition of electrospun TiO_2 nanorods for dye-sensitized solar. Nanotechnology. 2007;**18**:365709

[192] Kisumi T, Tsujiko A, Murakoshi K, Nakato Y. Crystal-face and illumination intensity dependences of the quantum efficiency of photoelectrochemical etching, in relation to those of water photooxidation, at *n*-TiO_2 (rutile) semiconductor electrodes. Journal of Electroanalytical Chemistry. 2003;**545**:99-107

[193] Lee H, Dregia S, Akbar S, Alhoshan M. Growth of 1-D TiO_2 nanowires on Ti and Ti alloys by oxidation. Journal of Nanomaterials. 2010;**7**. Article ID 503186

[194] Dinan B, Akbar S. One dimensional oxide nanostructures by gas-phase reaction. Functional Nanomaterials Letters. 2009;**2**:87-94

[195] Huo K, Zhang X, Fu J. Synthesis and filed emission properties of rutile TiO_2 nanowires arrays grown directly on a Ti metal self-source substrate. Journal of Nanoscience and Nanotechnology. 2009;**9**:3341-3346

[196] Daothong S, Songmee N, Thongtem S, Singjai P. Size-controlled growth of TiO_2 nanowires by oxidation of titanium substrates in the presence of ethanol vapor. Scripta Materialia. 2007;**57**:567-570

[197] Tan AW, Ismail R, Chua KH, Ahmad R, Akbar SA, Pingguan-Murphy B. Osteogenic potential of in-situ TiO_2 nanowire surfaces formed by thermal oxidation of titanium alloy surface. Applied Surface Science. 2014;**320**:161-170

[198] Pu Y-Ch, Wang G, Chang K-D, Ling Y, Lin Y-K, Fitzmorris BC, Liu Ch-M, Lu X, Tong Y, Zhang JZ, Yung-Jung Hsu Y-J, Li Y. Au Nanostructure-decorated TiO_2 nanowires exhibiting photoactivity across entire UV-visible region for photoelectrochemical water splitting. Nano Letters. 2013;**13**:3817-3823

[199] Stengl V, Bakardjieva S, Murafa N, Vecernıkova E, Subrt J, Balek V. Preparation and characterization of titania based nanowires. Journal of Nanoparticle Research. 2007;**9**:455-470